INFECTION AND IMMUNITY, Dec. 2005, p. 8397–8401 Vol. 73, No. 12
0019-9567/05/$08.00+0 doi:10.1128/IAI.73.12.8397–8401.2005

Toll-Like Receptor 2 Deficiency Delays Pneumococcal Phagocytosis and Impairs Oxidative Killing by Granulocytes

Maryse Letiembre,[1]† Hakim Echchannaoui,[1]† Philipp Bachmann,[1] Fabrizia Ferracin,[1] Concepción Nieto,[2] Manuel Espinosa,[2] and Regine Landmann[1]*

Division of Infectious Diseases, Department of Research, University Hospital, Hebelstrasse 20, CH-4031 Basel, Switzerland,[1] *and Centro de Investigaciones Biológicas, Consejo Superior de Investigaciones Científicas, Ramiro de Maeztu, 9, E-28040 Madrid, Spain*[2]

Received 23 July 2005/Accepted 5 August 2005

Phagocytosis and killing of *Streptococcus pneumoniae* was compared in blood-derived wild-type (WT) and Toll-like receptor 2 (TLR2)-deficient ($TLR2^{-/-}$) polymorphonuclear leukocytes (PMN). Phagocytosis of green fluorescent protein-transformed pneumococci was delayed in $TLR2^{-/-}$ PMN. These cells exhibited also a lower oxidative bactericidal activity against *S. pneumoniae* than WT PMN, suggesting that TLR2 modulates bacterial clearance in PMN.

The inflammatory response to purified lipoteichoic acid and membrane lipoproteins of gram-positive bacteria is dependent on Toll-like receptor 2 (TLR2) (3, 18). In contrast, inflammation, which follows infection with live gram-positive bacteria (1), is modulated only by TLR2. In addition to its effect on inflammation, TLR2 signaling also regulates phagocytosis. Indeed, macrophage phagocytosis of killed *Staphylococcus aureus* was found impaired in TLR2 and TLR4 double-knockout or MYD88KO macrophages in vitro (5). The contribution of TLR2 alone to granulocyte-dependent killing of live gram-positive bacteria remains unresolved. Previous reports from our group and others described that $TLR2^{-/-}$ mice have higher bacterial numbers in brain during meningitis than wild-type (WT) mice (10, 13). The reason for this defect in bacterial clearing is unknown. We found stronger adherence and uptake of *Streptococcus pneumoniae* to TLR2-deficient than to WT plexus choroideus epithelial cells 24 h after meningeal infection (9). This could be due to a weakened antimicrobial activity of TLR2-deficient phagocytes. Therefore, we investigated phagocytosis and bactericidal activity of WT and TLR2-deficient granulocytes against live *S. pneumoniae*.

Oxidative killing of *S. pneumoniae* by TLR2-deficient mouse blood PMN is reduced. Clinical isolates of *S. pneumoniae* serotype 3 (H_{14}) and serotype 1 (C5017) from patients with meningitis were used. H_{14} and C5017 had been applied for the murine meningitis model (9, 10). Bacteria were grown for 7 h in Todd-Hewitt broth supplemented with 0.5% Bacto yeast extract (Difco) and subcultured overnight in Mueller-Hinton broth double concentrated (MHB×2; Difco). The inoculum size used for incubation with polymorphonuclear leukocytes (PMN) (multiplicity of infection [MOI] of 1) was calculated from an optical density at 600 nm of 0.4 (4×10^7 CFU/ml). Each inoculum was retrospectively assessed by CFU counting on blood agar plates. PMN were isolated to a purity of >97% (Gr1 staining) and bactericidal activity was measured, with modifications of previously published methods (22, 23) from a blood pool of at least 3 mice. The average yield was 150,000 PMN/mouse. Briefly, PMN were resuspended with plasma-preopsonized H_{14} *S. pneumoniae* or C5017 and incubated at 37°C for 30 min. Control assays included the addition of 100 μg/ml of gentamicin after the incubation to confirm that remaining bacteria were extracellular.

After 30 min, killing by $TLR2^{-/-}$ cells was significantly lower than killing by WT cells (median 25% versus 60%, respectively) (Fig. 1A) ($P < 0.01$). Bacteria are killed by oxidative and nonoxidative mechanisms; the former requiring the enzyme NADPH oxidase, the activity of which can be blocked with diphenyleneiodonium (DPI) (11). To identify the mechanism of defective killing in $TLR2^{-/-}$ mice, bactericidal activity of WT and $TLR2^{-/-}$ PMN was compared in the presence of DPI. Oxidative killing was clearly failing in $TLR2^{-/-}$ mice, since DPI reduced killing by WT PMN and not by $TLR2^{-/-}$ cells (Fig. 1B). Alternatively, it can be hypothesized that the defect in killing of $TLR2^{-/-}$ cells was due to a lack of priming. PMN were pretreated with tumor necrosis factor before the bactericidal assay. This treatment did not increase the killing activity of $TLR2^{-/-}$ cells (data not shown). In conclusion, reduced oxidative bactericidal activity, which we found in vitro may have contributed to the increased bacterial load in $TLR2^{-/-}$ mice during meningitis. Our results support in vitro studies showing that TLR2 triggering with lipoteichoic acid or Pam_3CSK_4, induces or enhances fMLP-induced oxidative burst in human granulocytes (17, 21). The role of TLRs in oxidative burst generation is further documented for group B streptococci, as mice, which lack the common signal molecule MyD88, failed to produce reactive oxygen upon stimulation with these bacteria (12). Future studies will investigate the molecular mechanism of TLR2-mediated oxidative killing and in particular whether TLR2 activation affects translocation of NADPH oxidase or reduces superoxide anion scavenging.

Phagocytosis of green fluorescent protein (GFP)-*S. pneu-*

* Corresponding author. Mailing address: Division of Infectious Diseases, Department of Research, University Hospital, Hebelstrasse 20, CH-4031 Basel, Switzerland. Phone: 41-61-265 23 25. Fax: 41-61-265 32 72. E-mail: Regine.Landmann@unibas.ch.
† M.L. and H.E. contributed equally to this work.

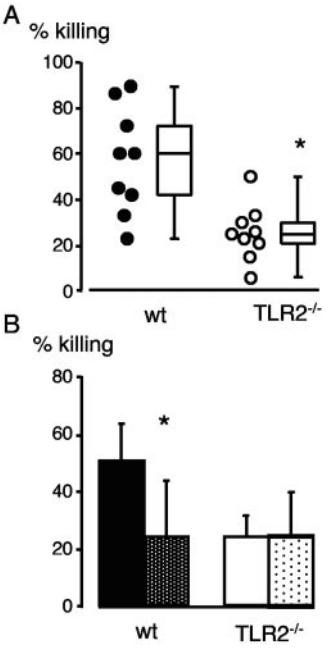

FIG. 1. Killing of encapsulated H_{14} *S. pneumoniae* by purified blood PMN. (A) WT and TLR2$^{-/-}$ PMN (2×10^5 cells) were incubated with plasma-preopsonized *S. pneumoniae* at an MOI of 1 for 30 min at 37°C. (B) Killing of H_{14} *S. pneumoniae* by PMN in the presence of the NADPH oxidase inhibitor DPI. PMN without DPI (black and white histograms) and PMN treated with DPI (dotted histograms). Mean values ± standard deviations from nine (A) and four (B) independent experiments (analysis of variance) are given (*, $P < 0.05$).

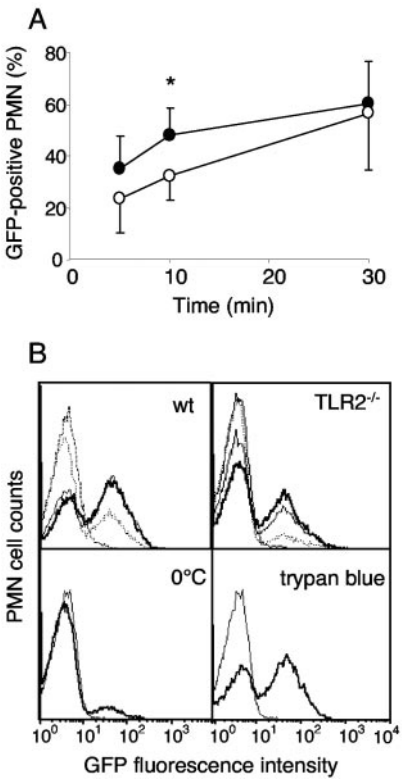

FIG. 2. (A) Time course of phagocytosis of GFP-C5017 *S. pneumoniae* by purified mouse blood PMN analyzed by FACS and expressed as the percentage of PMN containing GFP bacteria after 5, 10, and 30 min. WT PMN (black circles) and TLR2$^{-/-}$ PMN (open circles). Flow cytometry acquisition was gated on PMN cells based on their forward scatter/side scatter and viability (negative propidium iodide staining). Mean values ± standard deviations from five independent experiments. Paired samples of WT and TLR2$^{-/-}$ cells were compared with the nonparametric analysis of variance (*, $P < 0.05$). (B) Fluorescence histograms of GFP-positive PMN during phagocytosis. PMN incubated 5, 10, and 30 min (dotted line, thin solid line and thick solid line, respectively) at 37°C (upper histograms) and WT PMN incubated 10 min at 0°C (lower left histogram) or 10 min at 37°C adding trypan blue to quench extracellular GFP-*S. pneumoniae* (lower right histogram) are shown. C5017 WT control (dashed line in the upper histograms and thin solid line in the lower histograms) is also shown. One representative out of three experiments is shown.

***moniae* by TLR2-deficient mouse blood PMN is delayed.** Reduced bacterial killing may be due not only to weakened enzymatic activity but also to slowed phagocytosis. We therefore compared uptake of live GFP-*S. pneumoniae* by PMN from the two mouse strains by flow cytometry and confocal microscopy. *S. pneumoniae* serotype 1 (C5017) was transformed as previously described (6) with the plasmid pLS1GFP and competence stimulating peptide 1. The plasmid contained a mutated, soluble, and brightly fluorescent *gfp* gene (15, 7) under the control of the P_M promoter (16) and an erythromycin-resistant (Erm^r) gene. P_M directs transcription of the *malMP* operon, which is involved in maltose utilization within the pneumococcal *mal* regulon (14, 16). P_M is negatively regulated by the protein MalR, which is inactivated in the presence of maltose. Transformed C5017 similarly expressed GFP in the exponential and stationary growth phase; GFP expression was sustained even 2 days after removal of antibiotic from the culture medium as determined by fluorescence-activated cell sorter (FACS) analysis and confocal microscopy. The constitutive *gfp* expression in GFP-*S. pneumoniae* cultures may be explained by two circumstances. First, in plasmid pLS1GFP, P_M is negatively controlled by a single chromosomal copy of *malR* and thus not very tightly regulated. Second, this promoter is induced by a mixture of glucose and maltose (14). Maltose can be formed endogenously, at least in *Escherichia coli*, from glucose, independently of the maltose system enzymes (8). For phagocytosis, fluorescence was analyzed from the viable pure PMN population after incubation with shaking at 37°C, or at 4°C for controls, for 2.5 to 30 min at an MOI of 1 to 100 with GFP-C5017 *S. pneumoniae*. Bacteria were preopsonized for 30 min at 37°C with 10% fresh mouse hirudine-plasma and this plasma concentration was maintained during phagocytosis.

The kinetics of phagocytosis were significantly delayed in TLR2$^{-/-}$ as compared to WT PMN (Fig. 2). At an MOI of 10:1, the percentage of PMN containing GFP bacteria increased to a plateau value of 48.2 ± 9.9% within 10 min in WT cells, whereas the same value was obtained only after 30 min by TLR2$^{-/-}$ PMN (Fig. 2A) ($P < 0.05$). Phagocytosis did not further increase beyond 30 min in cells from either strain (data not shown). Figure 2B (upper FACS histograms) illustrates that, although the proportion of GFP-positive cells was smaller in TLR2$^{-/-}$ than WT cells, the mean fluorescence among

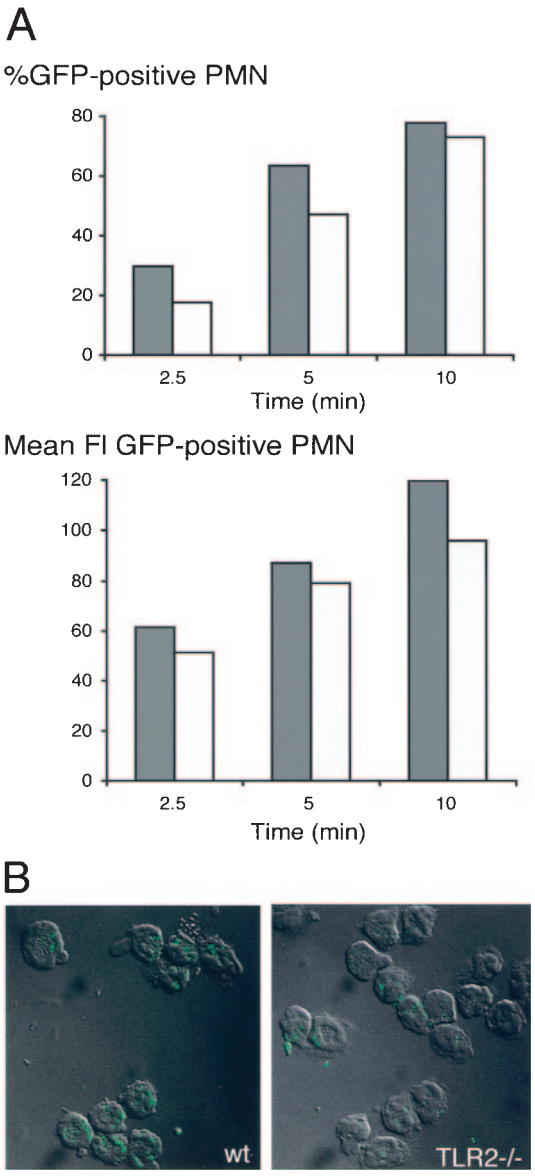

FIG. 3. (A) Percentage GFP-positive PMN and mean FI of GFP during phagocytosis by WT and TLR2$^{-/-}$ PMN. Plasma-opsonized GFP-C5017 *S. pneumoniae* cells were incubated at an MOI of 100:1 with WT (dark gray columns) and TLR2$^{-/-}$ (light gray columns) PMN for 2.5 to 10 min at 37°C and then washed, and the percentages of GFP-positive PMN (top panel) and mean FI (lower panel) of a scatter-gated viable PMN population were analyzed by FACS. One out of three similar experiments is shown. (B) Confocal micrography of GFP-C5017 *S. pneumoniae* phagocytosis by WT (left) and TLR2$^{-/-}$ (right) PMN after 2.5 min. Transmission micrographs of combined serial Z-stacks 0.5 μm thick showing PMN that have internalized GFP bacteria. Scale bars, 10 μm.

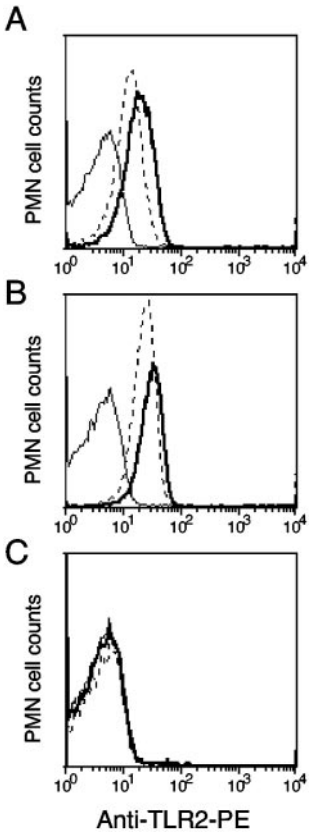

FIG. 4. Expression of TLR2 in purified blood PMN from WT (A and B) and TLR2$^{-/-}$ (C) mice. (A) TLR2 fluorescence after 10-min (dotted line) and 30-min (thick line) incubation of the cells at 37°C without phagocytosis. (B) TLR2 fluorescence after 10-min (dotted line) and 30-min (thick line) phagocytosis of GFP-positive bacteria at 37°C. (C) Staining of TLR2$^{-/-}$ PMN with TLR2 antibody during phagocytosis at 10 min (dotted line) and 30 min (thick line). All stainings included an isotype control antibody (thin line). One out of three similar experiments is shown.

GFP-positive PMN was similar in cells from both strains. The signal was specific, since at 0°C a very weak uptake (8%) was seen (Fig. 2B). The uptake was strictly dependent on complement, since it was absent, when bacteria had not been opsonized or preopsonized with frozen plasma or serum (data not shown). Moreover it was derived from intracellular bacteria, since it was maintained after quenching of extracellular fluorescence by trypan blue (Fig. 2B). The fluorescence results obtained at an MOI of 10:1 indicate that, while the fraction of phagocytosing PMN was smaller among TLR2$^{-/-}$ than among WT cells, the average numbers per cell of GFP molecules were similar in TLR2$^{-/-}$ and WT cells. In contrast, at an MOI of 100:1, when a large PMN fraction (80% after 10 min) (Fig. 3A) contained bacteria, the number of GFP molecules per cell was also clearly higher in the WT than in TLR2$^{-/-}$ PMN. This is illustrated in Fig. 3A as a higher mean fluorescence intensity (FI) in the WT than in TLR2$^{-/-}$ cells. These data were confirmed by confocal microscopy studies, which showed that the proportion of cells containing bacteria was higher in the WT than in TLR2$^{-/-}$ mice and more bacteria were contained within one cell. An example at 2.5 min at an MOI of 100:1 is illustrated in Fig. 3B. The delayed phagocytosis observed with TLR2$^{-/-}$ PMN could be explained by a defect of the TLR2$^{-/-}$ cells. However, a component of the TLR2$^{-/-}$ plasma could also contribute to inhibition of phagocytosis. Therefore phagocytosis was assessed in the WT and TLR2$^{-/-}$ PMN, which were incubated with plasma of either strain. Ten minutes after incubation, the percentage of GFP-positive cells was signifi-

cantly higher in WT than in TLR2$^{-/-}$ PMN, irrespective of the source of the opsonizing plasma (data not shown). This indicates that the delayed phagocytosis in TLR2$^{-/-}$ cells was due to a cellular defect. This defect was, however, effective only during the early phases and disappeared 30 min after initiation of the bacterial contact.

TLR2 expression in PMN increases with phagocytosis. The defect in phagocytosis observed in TLR2$^{-/-}$ PMN could be directly due to the absence of TLR2 expression in these cells or to another molecular change consequent to TLR2 deficiency. Therefore TLR2 expression was investigated in WT and TLR2-deficient resting and phagocytosing cells. TLR2 FACS analysis was performed by incubating PMN after phagocytosis with GFP-C5017 with phycoerythrin (PE)-labeled rat anti-mouse TLR2 antibody (clone 6C2; eBioscience, San Diego, CA) or the corresponding PE-labeled rat immunoglobulin G2b isotype control antibody. Ten and 30 min after incubation at 37°C without phagocytosis, 81 and 86% of blood PMN expressed membrane TLR2 with a mean FI of 16 and 22, respectively (Fig. 4A). The fraction of GFP-positive, TLR2-positive cells rose from 91 to 94%, and the mean FI increased from 26 to 32, 10 and 30 min after phagocytosis, respectively (Fig. 4B). Phagocytosing TLR2-deficient cells were negative in TLR2 staining (Fig. 4C). Fifty percent of resting PMN kept at 4°C were TLR2 positive (data not shown). Our results show that surface TLR2 increased with incubation at 37°C and that nearly all PMN had strong expression during phagocytosis. This is in agreement with recent data showing TLR2 expression in all murine PMN including functionally different subpopulations (19). Thus, TLR2 expression on PMN most likely contributed directly or indirectly to the acceleration of the uptake process. We could exclude the contribution of a plasma factor to the reduction of phagocytosis in TLR2$^{-/-}$ PMN, because bacterial opsonization and intracellular uptake by WT PMN in the presence of TLR2$^{-/-}$ plasma did not delay phagocytosis. We also found CR3 and Fc receptor expression of similar intensity in all WT and TLR2$^{-/-}$ PMN (data not shown).

Our findings are in contrast to a study in which internalization of zymosan by RAW macrophages was found independent of TLR2 (20). Our study utilizes live *S. pneumoniae* and PMN and thus more closely resembles the physiological situation and clearly shows that the absence of TLR2 had a negative effect on phagocytosis. With regard to the molecular mechanisms involved, the Rho GTPases Rac-1 and Cdc42 represent a possible target of TLR2 activation. It was previously shown that TLR2 stimulation by heat-killed *S. aureus* in vitro induces a rapid activation of Rac-1 and Cdc42 (4), which are both required for actin assembly during phagocytosis (2). In a recent study, phagosome maturation was found impaired in the absence of TLR signaling in mouse macrophages infected with heat-killed *S. aureus* (5). This TLR-induced phagosome maturation was found to occur via MyD88-dependent activation of the p38 MAP kinase pathway. It remains unknown whether the effect of TLR2 on pneumococcal killing is the consequence of its effect on actin polymerization and PMN phagocytosis.

In conclusion, our studies clearly demonstrate that killing and phagocytosis of *S. pneumoniae* by mouse PMN were impaired in the absence of TLR2. These defects might explain the higher bacterial load observed in brains of TLR2$^{-/-}$ mice during meningitis (10).

We thank Zarko Rajacic and Beat Erne for technical help, Gennaro De Libero and Therese Resink for critically reading the manuscript, Donald A. Morrison of Chicago, IL, for his generous gift of CSP, Gerd Pluschke from the Swiss Tropical Institute (Basel, Switzerland) for his kind gifts of *S. pneumoniae* strain C5017.

This work was supported by the Novartis-Stiftung (to R.L.), National Science Foundation grants 32-63855.00 and 3100 AO-104259/1; by Ministerio de Educación y Ciencia (grants BMC2002-11562-E and BFU2004-00687/BMC); and by Instituto de Salud Carlos III, network REIPI-FIS-CO 3/14 (to M.E.).

REFERENCES

1. **Aderem, A., and R. J. Ulevitch.** 2000. Toll-like receptors in the induction of the innate immune response. Nature **406:**782–787.
2. **Aderem, A., and D. M. Underhill.** 1999. Mechanisms of phagocytosis in macrophages. Annu. Rev. Immunol. **17:**593–623.
3. **Aliprantis, A. O., R. B. Yang, M. R. Mark, S. Suggett, B. Devaux, J. D. Radolf, G. R. Klimpel, P. Godowski, and A. Zychlinsky.** 1999. Cell activation and apoptosis by bacterial lipoproteins through toll-like receptor-2. Science **285:**736–739.
4. **Arbibe, L., J. P. Mira, N. Teusch, L. Kline, M. Guha, N. Mackman, P. J. Godowski, R. J. Ulevitch, and U. G. Knaus.** 2000. Toll-like receptor 2-mediated NF-kappa B activation requires a Rac1-dependent pathway. Nat. Immunol. **1:**533–540.
5. **Blander, J. M., and R. Medzhitov.** 2004. Regulation of phagosome maturation by signals from toll-like receptors. Science **304:**1014–1018.
6. **Bricker, A. L., and A. Camilli.** 1999. Transformation of a type 4 encapsulated strain of Streptococcus pneumoniae. FEMS Microbiol. Lett. **172:**131–135.
7. **Cormack, B. P., R. H. Valdivia, and S. Falkow.** 1996. FACS-optimized mutants of the green fluorescent protein (GFP). Gene **173:**33–38.
8. **Decker, K., R. Peist, J. Reidl, M. Kossmann, B. Brand, and W. Boos.** 1993. Maltose and maltotriose can be formed endogenously in *Escherichia coli* from glucose and glucose-1-phosphate independently of enzymes of the maltose system. J. Bacteriol. **175:**5655–5665.
9. **Echchannaoui, H., P. Bachmann, M. Letiembre, M. Espinosa, and R. Landmann.** 2005. Regulation of Streptococcus pneumoniae distribution by Toll-like receptor 2 in vivo. Immunobiology **210:**229–236.
10. **Echchannaoui, H., K. Frei, C. Schnell, S. L. Leib, W. Zimmerli, and R. Landmann.** 2002. Toll-like receptor 2-deficient mice are highly susceptible to Streptococcus pneumoniae meningitis because of reduced bacterial clearing and enhanced inflammation. J. Infect. Dis. **186:**798–806.
11. **Hampton, M. B., A. J. Kettle, and C. C. Winterbourn.** 1996. Involvement of superoxide and myeloperoxidase in oxygen-dependent killing of *Staphylococcus aureus* by neutrophils. Infect. Immun. **64:**3512–3517.
12. **Henneke, P., O. Takeuchi, R. Malley, E. Lien, R. R. Ingalls, M. W. Freeman, T. Mayadas, V. Nizet, S. Akira, D. L. Kasper, and D. T. Golenbock.** 2002. Cellular activation, phagocytosis, and bactericidal activity against group B streptococcus involve parallel myeloid differentiation factor 88-dependent and independent signaling pathways. J. Immunol. **169:**3970–3977.
13. **Koedel, U., B. Angele, T. Rupprecht, H. Wagner, A. Roggenkamp, H. W. Pfister, and C. J. Kirschning.** 2003. Toll-like receptor 2 participates in mediation of immune response in experimental pneumococcal meningitis. J. Immunol. **170:**438–444.
14. **Lacks, S.** 1968. Genetic regulation of maltosaccharide utilization in Pneumococcus. Genetics **60:**685–706.
15. **Miller, W. G., and S. E. Lindow.** 1997. An improved GFP cloning cassette designed for prokaryotic transcriptional fusions. Gene **191:**149–153.
16. **Puyet, A., A. M. Ibanez, and M. Espinosa.** 1993. Characterization of the Streptococcus pneumoniae maltosaccharide regulator MalR, a member of the LacI-GalR family of repressors displaying distinctive genetic features. J. Biol. Chem. **268:**25402–25408.
17. **Sabroe, I., L. R. Prince, E. C. Jones, M. J. Horsburgh, S. J. Foster, S. N. Vogel, S. K. Dower, and M. K. Whyte.** 2003. Selective roles for Toll-like receptor (TLR)2 and TLR4 in the regulation of neutrophil activation and life span. J. Immunol. **170:**5268–5275.
18. **Schwandner, R., R. Dziarski, H. Wesche, M. Rothe, and C. J. Kirschning.** 1999. Peptidoglycan- and lipoteichoic acid-induced cell activation is mediated by toll-like receptor 2. J. Biol. Chem. **274:**17406–17409.
19. **Tsuda, Y., H. Takahashi, M. Kobayashi, T. Hanafusa, D. N. Herndon, and F. Suzuki.** 2004. Three different neutrophil subsets exhibited in mice with different susceptibilities to infection by methicillin-resistant Staphylococcus aureus. Immunity **21:**215–226.
20. **Underhill, D. M., A. Ozinsky, A. M. Hajjar, A. Stevens, C. B. Wilson, M. Bassetti, and A. Aderem.** 1999. The Toll-like receptor 2 is recruited to

macrophage phagosomes and discriminates between pathogens. Nature **401:** 811–815.
21. **von Aulock, S., S. Morath, L. Hareng, S. Knapp, K. P. van Kessel, J. A. van Strijp, and T. Hartung.** 2003. Lipoteichoic acid from Staphylococcus aureus is a potent stimulus for neutrophil recruitment. Immunobiology **208:**413–422.
22. **Zimmerli, W., B. Seligmann, and J. I. Gallin.** 1986. Exudation primes human and guinea pig neutrophils for subsequent responsiveness to the chemotactic peptide N-formylmethionylleucylphenylalanine and increases complement component C3bi receptor expression. J. Clin. Investig. **77:**925–933.
23. **Zimmerli, W., F. A. Waldvogel, P. Vaudaux, and U. E. Nydegger.** 1982. Pathogenesis of foreign body infection: description and characteristics of an animal model. J. Infect. Dis. **146:**487–497.

Editor: J. N. Weiser